Comparative study of the interaction in the $pp\eta$ and $pp\eta'$ systems

COSY–11 Collaboration

IKP, Forschungszentrum Jülich, D-52425 Jülich, Germany
ZEL, Forschungszentrum Jülich, D-52425 Jülich, Germany
Institute of Physics, Jagellonian University, PL-30-059 Cracow, Poland
IKP, Westfälische Wilhelms–Universität, D-48149 Münster, Germany
Institute of Nuclear Physics, PL-31-342 Cracow, Poland
Institute of Physics, University of Silesia, PL-40-007 Katowice, Poland

Spokesperson: P. Moskal

Abstract

We would like to continue the comparative study of the interactions of the η and η' mesons with protons as suggested in the already accepted COSY Proposal No. 11.7 titled "Study of proton-η' and proton-η interaction". The first part of these investigations, namely the study of the proton-η interaction, is finished. Here we present results of the completed evaluation of the high statistics measurement of the $pp \to pp\eta$ reaction performed at the COSY-11 facility during the beam-time which had been assigned in the frame of that proposal. Qualitative phenomenological analysis of the determined differential distributions for the production cross sections revealed an enhancement of the population density in the kinematical regions corresponding to the low proton-η relative momentum. The effect is too large to be described by the on-shell incoherent pairwise interaction among the produced particles and its understanding will require a rigorous three-body approach to the $pp\eta$ system. At present many theoretical groups are seeking an explanation of this intriguing observation [1].

Encouraged by this finding we intend now to realize the second part of the Proposal No. 11.7, that is to investigate the interaction of the meson η' with protons. Additionally to the originally presented motivation for the study of the low energy $pp\eta'$ system we argue that the comparison of the differential cross sections of the $pp \to pp\eta'$ and $pp \to pp\eta$ reactions combined with the shape of the excitation functions will facilitate to disentangle between the contributions from the higher partial waves and the proton-proton-meson interactions for both produced systems.

In the close to threshold excitation function for the $pp \to pp\eta'$ reaction a signal from the proton-η' force has not been observed. Thus, the determination of the distributions of the invariant masses for two-particle subsystems of the $pp\eta'$ final state could give the first ever experimental evidence for this still completely unknown interaction. In the case of the $pp\eta$ system these observables proved to be very sensitive to the proton-η interaction. Their determination would also strengthen significantly constraints on the analysis aiming at the determination of contributions from mesonic, gluonic, nucleonic and resonance currents to the production process. Therefore, we ask for **4 weeks** of COSY beam-time in the coming period in order to determine differential distributions of the cross section for the $pp \to pp\eta'$ reaction at Q = 15.5 MeV, the same excess energy at which the corresponding spectra for the $pp \to pp\eta$ reaction have been determined.

1 Manifestation of the η-p-p and η′-p-p interaction

In the last decade large experimental as well as theoretical efforts were concentrated on the study of the creation of η and η′ mesons via the hadronic interactions. Measurements of the production of these mesons in the elementary nucleon-nucleon collision have been performed in the vicinity of the kinematical threshold where only one partial wave in both initial - and final state is expected to contribute to the production process. For example in case of the proton-proton collision the dominance of the ${}^3P_0 \rightarrow {}^1S_0 s$ transition is expected up to an excess energy of about 40 MeV and 100 MeV for η and η′ meson, respectively [2]. This simplifies significantly the interpretation of the data, yet still appears to be challenging due to the three particle final state system with a complex hadronic potential.

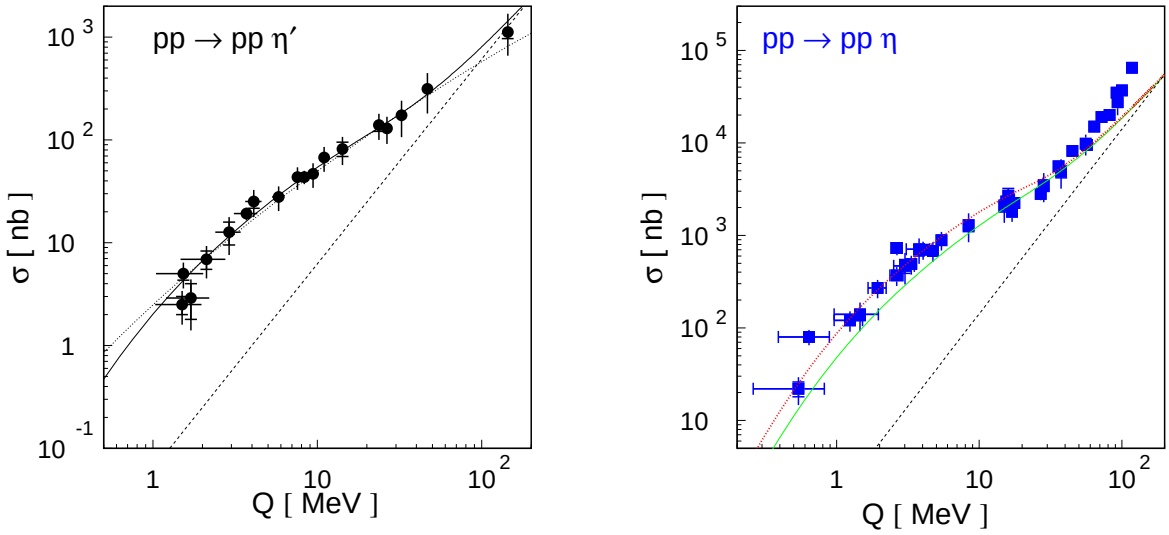

Figure 1: **(left)** Total cross section for the $pp \rightarrow pp\eta'$ reaction as a function of the centre–of–mass excess energy Q. Data are from refs. [3, 4]. The solid line shows the phase–space distribution with inclusion of proton–proton strong and Coulomb interactions.
The dotted line indicates the parametrization of reference [6] with $\varepsilon = 0.3$ and the dashed line indicates a phase–space integral normalized arbitrarily.
(right) Total cross section for the $pp \rightarrow pp\eta$ reaction as a function of the centre–of–mass excess energy Q. Data are from refs. [4, 5]. The dashed line indicates a phase–space integral normalized arbitrarily. The phase–space distribution with inclusion of proton–proton strong and Coulomb interactions fitted to the data in the excess energy range between 15 and 40 MeV is shown as the solid line. Additional inclusion of the proton–η interaction is indicated by the dotted line. The scattering length $a_{p\eta} = 0.7\,\mathrm{fm} + i\,0.4\,\mathrm{fm}$ and the effective range parameter $b_{p\eta} = -1.50\,\mathrm{fm} - i\,0.24\,\mathrm{fm}$ [7] have been arbitrarily chosen.

The determined energy dependences of the total cross section for η′ [3, 4] and η [4, 5] mesons in proton-proton collisions are presented in figure 1. Comparing the data to the arbitrarily normalized phase-space integral (dashed lines) reveals that the proton-proton FSI enhances the total cross section by more than an order of magnitude for low excess energies. One recognizes also that in the case of the η′ the data are described very well (solid line) assuming that the on-shell proton-proton amplitude exclusively determines the phase-space population. This indicates that the proton-η′ interaction is too small to manifest itself in the excitation function within the presently achievable accuracy. In the case of the η meson the increase of the total cross section for very low and very

high energies is much larger than expected from the final state interaction between protons. The excess at higher energies can be assigned to the onset of higher partial waves, and the enhancement at threshold can be plausibly explained by the influence of the attractive interaction between the η meson and the proton.
A quantitative derivation of the $p-\eta$ and $p-\eta'$ hadronic potentials requires, however, a sophisticated theoretical treatment since the distortion caused by the nucleons is by at least an order of magnitude larger than that due to the meson–nucleon forces, and even small fractional inaccuracies in the description of nucleon–nucleon effects may obscure the inference on the meson–nucleon interaction. To minimize the ambiguities which may result from these discrepancies – at least for the qualitative estimation of the effects of the unknown meson–nucleon interaction – one can compare the spectra from the production of a meson under investigation to the spectra determined for the production of a meson whose interaction with nucleons is well established. To visualize the influences of the $p-\eta$ and $p-\eta'$ interaction on the energy dependence of the total cross section we have compared the modulus of the primary transition amplitude $|M_0|$ of the $pp \to pp\eta$ and $pp \to pp\eta'$ reactions to the one extracted from the data on the $pp \to pp\pi^0$ reaction [8] [1].

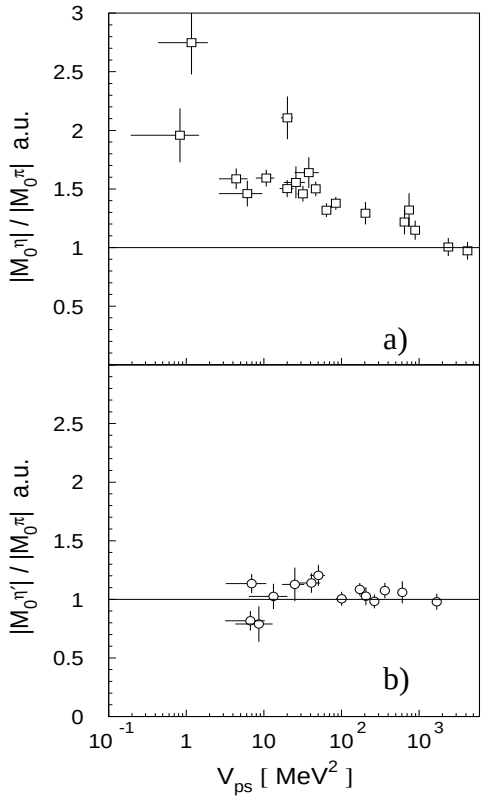

Figure 2: The ratios of a) $|M_0^{\eta}|/|M_0^{\pi^0}|$ and b) $|M_0^{\eta'}|/|M_0^{\pi^0}|$ extracted from the experimental data for $pp \to pp\eta$ [5] and $pp \to pp\eta'$ [3] reactions. $|M_0^{\pi^0}|$ was calculated by interpolating the data of reference [11]. The figure is adapted from reference [8].

Figures 2a and 2b show the dependence of $|M_0|$ on the phase–space volume for η and η' production normalized to $|M_0^{\pi^0}|$. The values of $|M_0|$ were extracted from the experimental data disregarding the proton–meson interaction. If the influence of the neglected interactions were the same in the case of the η (η') and π^0 production the points would be consistent with the solid line. This holds in case of the $pp \to pp\eta'$ reaction indicating the weakness of the proton–η' interaction independently of the prescription used for the proton–proton FSI [8]. In case of the η' meson its low–energy interaction with the nucleons was expected to be very weak since there exists no

[1] The S-wave π-proton interaction is negligibly weak in comparison to the proton-proton one. The real part of the $\pi - p$ scattering length ($|a_{p\pi}| = 0.13$ fm [9]) is more than a factor of 50 smaller than $|a_{pp}| = 7.83$ fm [10].

baryonic resonance which would decay into $N\eta'$ channel [12]. In contrary, the existence of the $N^*(1535)$ resonance, which decays significantly into nucleon and the η meson, indicates that the $N\eta$ interaction is much stronger than the $N\eta'$ one, and indeed as depicted in figure 2a the strong effects of the ηpp FSI at low V_{ps} are visible. A similar effect is also observed in the photoproduction of η via the $\gamma d \to pn\eta$ reaction [13] indicating to some extent that the phenomenon is independent of the production process but is rather related to the interaction among the η meson and nucleons in the $S_{11}(1535)$ resonance region.

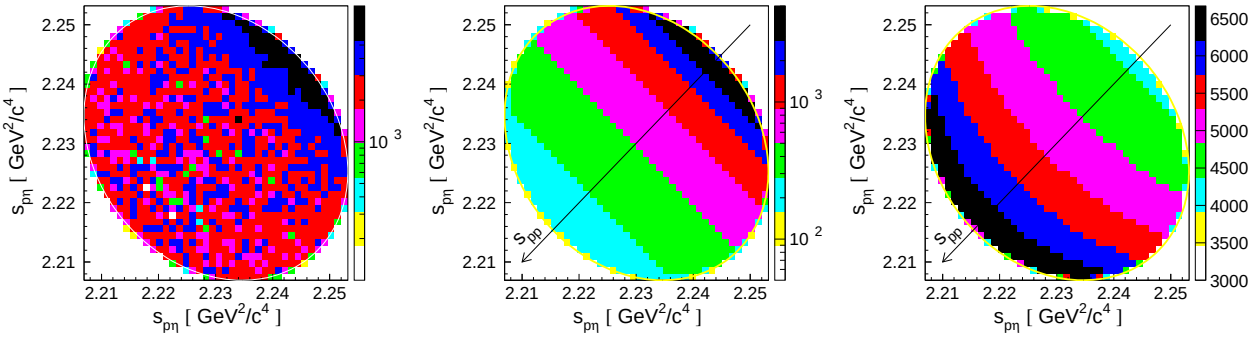

Figure 3: **(left)** Dalitz plot distributions corrected for the detection acceptance and efficiency as determined for the $pp \to pp\eta$ reaction at Q = 15.5 MeV.
(middle) Monte-Carlo simulations for the $pp \to pp\eta$ reaction at Q = 15.5 MeV: Phase-space density distribution modified by the proton - proton final state interaction.
(right) Simulated phase-space density distribution modified by the proton-η interaction, with a scattering length $a_{p\eta}$ = 0.7 fm + i 0.3 fm. Details of the calculations together with the discussion of the nucleon-nucleon and nucleon-meson final-state-interaction can be found in reference [2].
Lines surrounding plots depict the kinematical limits.

The interaction between particles depends on their relative momenta or equivalently on the invariant masses of the two-particle subsystems. Therefore it should show up as modifications of the phase-space abundance in the kinematics regions where the outgoing particles possess small relative velocities. Only two invariant masses of the three subsystems are independent and therefore the entire principally accessible information about the final state interaction of the three-particle systems can be presented in the form of the Dalitz plot. Figure 3(left) indicates the event distribution as determined experimentally for the $pp\eta$ system at an excess energy of Q = 15.5 MeV. In the figures one easily recognizes the growths of the population density at the region where the protons have small relative momenta which can be assigned to the strong attractive S-wave interaction between the protons. This is qualitatively in agreement with the expectation presented in figure 3(middle), which shows results of the Monte-Carlo calculations where the homogenously populated phase space was weighted by the squre of the on-shell $^1S_0$ proton-proton scattering amplitude. However, already at this two dimensional representation it is visible that the experimentally determined distribution remains rather homogeneous outside the region of the small proton-proton invariant masses, whereas the simulated abundance decreases gradually with the growing s_{pp} (as indicated by the arrow). Figure 3(right) shows the simulated phase-space density distribution disregarding the proton–proton interaction but accounting for the interaction between the η–meson and the proton. Due to the lower strength of this interaction the expected deviations from a uniform distribution is by about two orders of magnitude smaller, yet an enhancement of the density

in the range of low invariant masses of proton–η subsystems is clearly visible. Please note that the scale in that figure is linear whereas in the middle and left panel the number of entries is shown logarithmically. Due to weak variations of the proton–η scattering amplitude the enhancement originating from the η–meson interaction with one proton is not separated from the η–meson interaction with the second proton. Therefore an overlapping of broad structures occurs. It is observed that the occupation density grows slowly with increasing s_{pp} opposite to the effects caused by the S–wave proton–proton interaction, yet similar to the modifications expected for the P–wave [14]. From the above example it is obvious that only in experiments with high statistics, signals from the meson–nucleon interaction can be observed over the overwhelming nucleon–nucleon final state interaction.

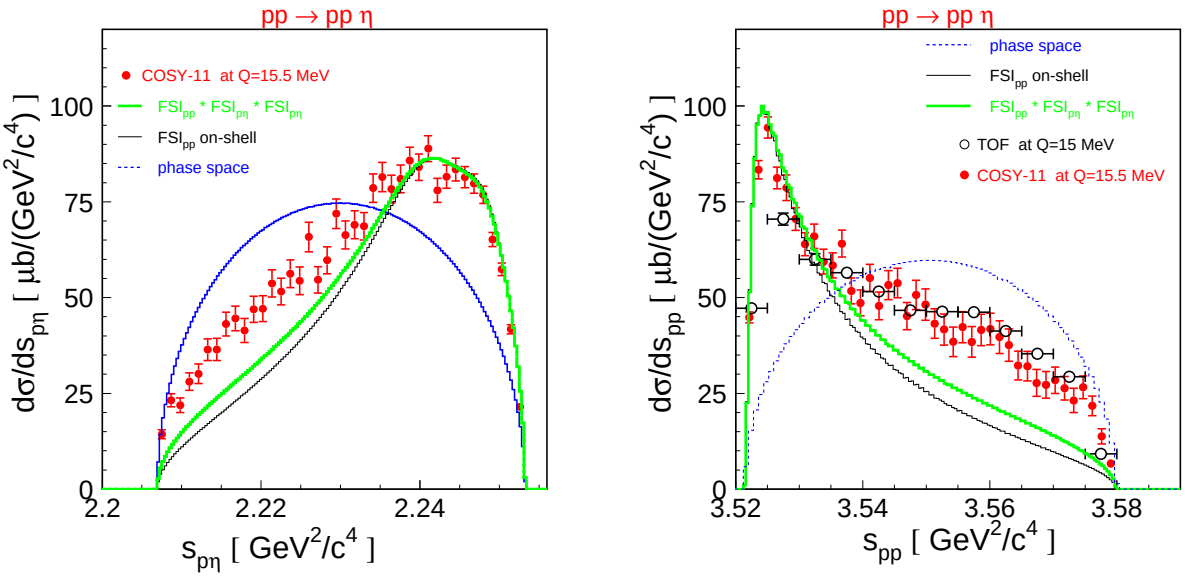

Figure 4: Distributions of the square of the proton-proton (s_{pp}) and proton-η ($s_{p\eta}$) invariant masses determined experimentally for the $pp \to pp\eta$ reaction at the excess energy of Q = 15.5 MeV by the collaborations COSY-11 (closed circles) and TOF [15] at Q = 15 MeV (open circles). The TOF data have been normalized to give the same total cross section as those of the COSY-11 since they are published in the arbitrary units. The integrals of the phase space weighted by the square of the proton-proton on-shell scattering amplitude (thin black lines)–FSI_{pp}, and by the product of FSI_{pp} and the square of the proton-η scattering amplitude (thick green lines), have been normalized arbitrarily at small values of s_{pp}. The thick green line was obtained assuming a scattering length of $a_{p\eta}$ = 0.7 fm + i 0.4 fm. The expectation under the assumption of the homogeneously populated phase space are shown as dotted blue curves.

A deviation of the experimentally observed population of the phase-space from the expectation based on the mentioned assumptions is even better visible in figure 4. This figure presents the projection of the phase-space distribution onto the s_{pp} axis corresponding to the axis indicated by the arrows in the two parts of figure 3. The superimposed lines in figure 4 correspond to the calculations performed under the assumption that the production amplitude can be factorized into primary production and the final state interaction. The thin solid lines depict calculations where only the proton-proton FSI was taken into account, whereas the green thick lines present results where the overall enhancement was factorized into the corresponding pair interactions of the $pp\eta$ system. The enhancement factor accounting for the proton-proton FSI has been calculated as a square of the on-shell proton-proton scattering amplitude derived according to the modified Cini-Fubini-Stanghellini formula including the Wong-Noyes Coulomb corrections [16, 8, 2]. The homogeneous phase-space

distribution (blue dotted lines) deviate strongly from the experimentally determined spectra. The curves with the inclusion of the proton-proton and proton-η FSI reflects the shape of the data for small invariant masses of the proton-proton system, yet they deviate significantly for large s_{pp} and small $s_{p\eta}$ values. An explanation for this discrepancy could be a contribution from P-wave proton-proton interaction [17], a significant influence of the off-shell effects of the interaction between outgoing particles or the possibly wrong assumption that proton-η and proton-proton interaction modify the phase space occupations only as incoherent weights.

In fact a little better description is achieved when the proton-proton interaction is accounted for by the realistic nucleon-nucleon potential which take into account the off-shell effects of the interacting particles (see dashed and blue solid line in figure 5). Figure 5 depicts the results obtained using two different models for the production process [18, 17].

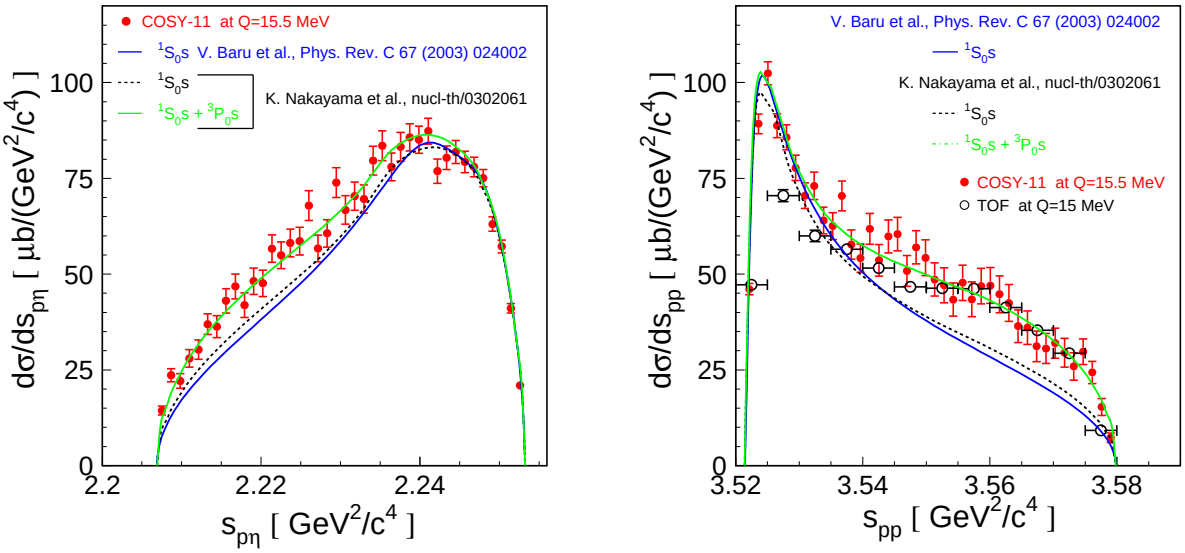

Figure 5: Distributions of the square of the proton-proton (s_{pp}) and proton-η ($s_{p\eta}$) invariant masses for the $pp \to pp\eta$ reaction at an excess energy of Q = 15.5 MeV. The data obtained by the TOF collaboration [15](open circles) have been normalized in magnitude to the results of the COSY-11 collaboration (closed circles). Blue solid and black dashed lines corresponds to the calculations under assumption of the $^3P_0 \to^1 S_0s$ transition according to the models described in references [18] and [17], respectively. Green lines shows the result after the addition of the $^1S_0 \to^3 P_0s$ contribution as suggested by Nakayama et al. [17].

The calculations for the $^3P_0 \to^1 S_0s$ transition differ slightly, yet the differences between the models are by far smaller then the observed signal. Therefore we can safely claim that the discussed effect is rather too large to be caused by the off-shell effects of the FSI between produced protons.

As can be seen in figure 6(right) the distributions of the η polar angle in the center of mass frame is fully isotropic (see figure 6). This is the next evidence – besides the shape of the excitation function and the kinematical arguments discussed in reference [2] – that at this excess energy (Q = 15.5 MeV) the η meson is produced in the center of mass frame predominantly with the angular momentum equal to zero. Similarly the distribution determined for the the polar angle of the relative proton-proton momentum with respect to the momentum of the η meson as seen in the di-proton rest frame is also isotropic. Yet, this does not imply directly that the relative angular momentum between protons is equal to zero, since protons posses an internal spin equal to $\frac{1}{2}$. Therefore, the contribution from the P-wave proton-proton system produced via the $^1S_0 \to^3 P_0s$

transition cannot be excluded. The isotropic angular distribution, as pointed out in reference [17] can also be principally achieved by the destructive interference between the transitions ${}^1S_0 \rightarrow {}^3P_0 s$ and ${}^1D_2 \rightarrow {}^3P_2 s$.

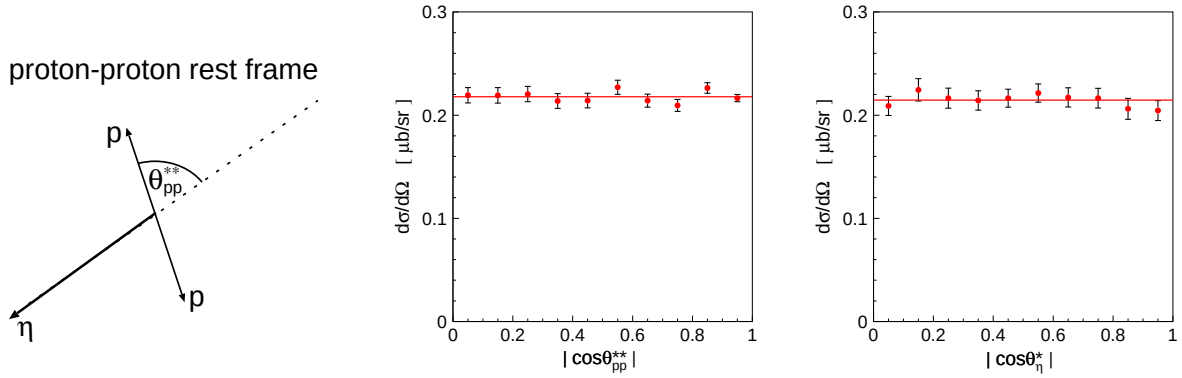

Figure 6: **(left)** Definition of the angle used in the middle figure.
(middle) Distribution of the polar angle of the relative proton-proton momentum with respect to the momentum of the η meson as seen in the di-proton rest frame. **(right)** Differential cross section of the $pp \rightarrow pp\eta$ reaction as a function of the η meson centre-of-mass polar angle.
Full circles in the middle and right panel depict experimental results for the $pp \rightarrow pp\eta$ reaction measured at Q = 15.5 MeV by the COSY-11 collaboration.

Nakayama and co-workers show that the invariant mass distributions can be very well described by the inclusion of the higher partial-wave amplitudes [17]. In fact, as depicted by the green lines in figures 5, an admixture of the ${}^1S_0 \rightarrow {}^3P_0 s$ transition leads to the excellent agreement with the experimentally determined invariant mass spectra. However, at the same time it leads to strong discrepancies in the shape of the excitation function. Whereas it describes the data points in the excess energy range between 40 MeV and 100 MeV it underestimate the total cross section below 20 MeV by a factor of 3.

From the above presented consideration we tend to induce that the discussed effect is due to interactions within the proton-proton-η system rather then to contributions from higher partial waves or off-shell effects of the proton-proton potential. Explanation of this finding remains at present a challenge for the theory since it requires a rigorous three-body approach to the system with the complex potentials.

On the experimental side it is natural to ask whether the structure observed in the invariant mass spectra will also appear in case of the production of other mesons. Specifically in the case of mesons which interactions with nucleons is significantly weaker. Especially intersting in that context are the mesons π^0 and η', the SU(3) flavour neutral partners of the meson η. We have chosen for the comparison the η' meson because of three reasons.
Firstly, since the interaction of the η' meson with nucleons is still quantitatively not established, though there are strong experimental indications that it is much weaker that the one between nucleon and η, just to name the fact that none of the baryon resonances deexcites via the emission of the η' meson. Thus the observation of the signal originating from the proton-η' interaction in the invariant mass distribution would be already exciting in itself. Secondly, because the η' meson is much heavier than the pion and the relevant angular momenta in the ppη' system are expected to be zero at Q = 15.5 MeV, whereas at this energy the $pp\pi^0$ system has significant contribution from Pp, Ps and Sd partial waves [19, 20, 21]. Thirdly, because the COSY-11 acceptance is much larger

for the $pp \to pp\eta'$ reaction than for the $pp \to pp\pi^0$ due to the large difference between the velocity of the center of mass systems of those reactions.

2 Report on the data analysis – in short

Using the COSY-11 detection system [22], utilizing a stochastically cooled proton beam of the cooler synchrotron COSY [23] and a hydrogen cluster target [24], we have performed a high statistics measurement of the $pp \to pp\eta$ reaction at an excess energy of Q = 15.5 MeV. The experiment was based on the four-momentum registration of both outgoing protons, whereas the η meson was identified via the missing mass technique.

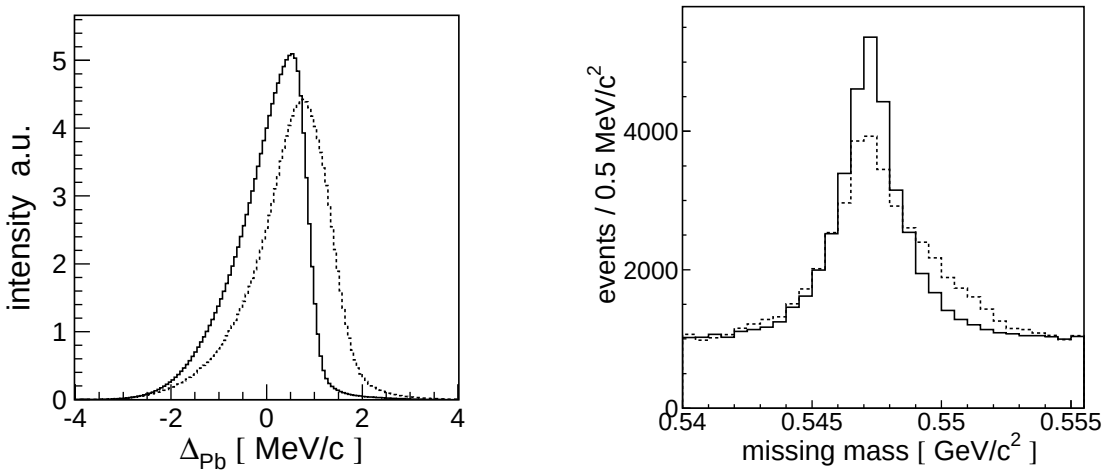

Figure 7: **(left)** The dashed curve denotes the difference of the measured proton beam momentum distribution from its nominal value of 2.027 GeV averaged over the whole measurement period. The solid line shows the beam momentum distribution after the correction for the mean value which was determined in 10 second intervals.
(right) Missing mass distribution for the $pp \to ppX$ reaction determined by means of the COSY-11 detection system at a beam momentum of 2.027 GeV. The solid histogram presents the data corrected for effects of the time dependent relative shifts between the beam and the target using the method described in reference [25]. The dashed histogram shows the result before the correction.

As a first step of the analysis the data were corrected for the mean beam momentum changes (see Fig. 7(left)) determined from the Schottky frequency spectra and the known beam optics. Next, from the distributions of the elastically scattered protons, the Schottky frequency spectrum, and the missing mass distribution of the $pp \to ppX$ reaction, using a method described elsewhere [25], we have estimated that for the measurement under discussion the spread of the beam momentum, the reaction points in horizontal and vertical direction amount to $\sigma(p_{beam}) = 0.63 \pm 0.03$ MeV/c, $\sigma(x) = 0.22 \pm 0.02$ cm, and $\sigma(y) = 0.38 \pm 0.04$ cm, respectively.

Comparison of the experimentally determined momentum spectra of the elastically scattered protons with the distributions simulated with different beam and target conditions allows us to established the position at which the beam crosses the target with an accuracy of 0.25 mm [25]. Accounting for the variation of the relative beam and target settings during the experiment we improved the missing mass resolution as demonstrated in figure 7(right). After subtraction of the multi pion production background (see figure 8), from the position of the peak on the missing mass spectrum we determined the actual absolute beam momentum to be $p_{beam} = 2.0259\,\text{GeV/c} \pm 0.0013\,\text{GeV/c}$,

which differs only slightly from the nominal value of $p_{beam}^{nominal} = 2.027$ GeV/c. The background was simulated taking into account $pp \to ppX$ reactions with $X = 2\pi$, 3π and 4π. Since we consider here only the very edge of the phase space distribution where the protons are produced predominantly in the S-wave the shape of the background can be reproduced assuming that the homogenous phase space distribution is modyfied only by the interaction between protons. Indeed, as can be observed in figure 8 the simulation describes the data very well. The calculated spectrum is hardly distinguishable from the real data.

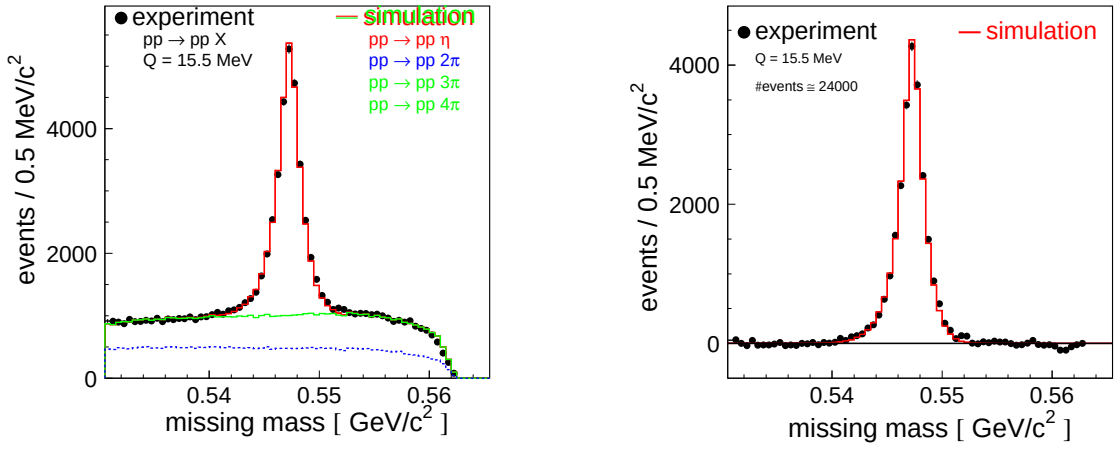

Figure 8: **(left)** Missing mass spectrum for the $pp \to ppX$ reaction determined in the experiment at the beam momentum of 2.0259 GeV/c. The mass resolution amounts to 1 MeV/c^2(σ). The superimposed histograms present the simulation for $1.5 \cdot 10^8$ events of the $pp \to pp\eta$ reaction, and 10^{10} events for the reactions $pp \to pp2\pi$, $pp \to pp3\pi$ and $pp \to pp4\pi$. The simulated histograms were fitted to the data varying only the magnitude. The fit resulted in 24009 ± 210 events with the production of the η meson. **(right)** Missing mass distribution after subtraction of the background.

2.1 Covariance matrix and kinematical fitting

As already mentioned in the previous section at the COSY-11 facility the identification of the $pp \to pp\eta$ reaction is based on the measurement of the momentum vectors of the outgoing protons and the utilisation of the missing mass technique. Inaccuracy of the momentum determination manifests itself in the population of kinematically forbidden regions of the phase space, preventing the precise comparison of the theoretically derived and experimentally determined differential cross sections. Figure 9(left) visualizes this effect and clearly demonstrates that the data scatter significantly outside the kinematically allowed region, in spite of the fact that the precision of the fractional momentum determination in the laboratory system ($\sigma(p_{lab})/p_{lab} \approx 7 \cdot 10^{-3}$) is quite high. Therefore, when seeking for small effects like for example the influence of the proton-η interaction on the population density of the phase-space, one needs either to fold theoretical calculations with the experimental resolution, or to perform the kinematical fitting of the data. Both procedures require the knowledge of the covariance matrix, and thus its determination constitutes a necessary step in the differential analysis and interpretation of the $pp \to pp\eta$ reaction measured with high statistics ($\approx$ 24000 events) at Q = 15.5 MeV.

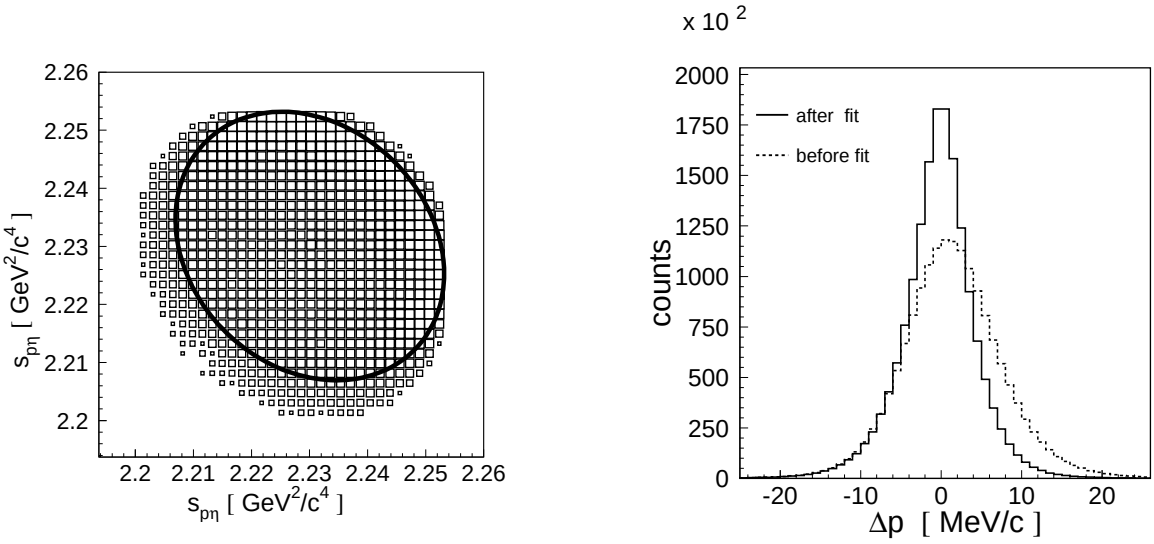

Figure 9: **(left)** Dalitz plot distribution of the $pp \to pp\eta$ reaction simulated at Q = 15.5 MeV. The number of entries is shown in a logarithmic scale. The solid line depicts the kinematically available area. **(right)** Spectrum of differences between reconstructed and generated absolute momentum of protons, as determined before (dashed line) and after kinematical fit (solid line).
Both pictures show results obtained taking into account the experimental conditions as described in the text.

In order to derive the covariance matrix we need to recognize and quantify all possible sources of errors in the reconstruction of the proton momenta. The four dominant effects are: i) multiple scattering in the dipole exit foil, air and detectors, ii) finite resolution of the position determination of the drift chambers, iii) finite distributions of the beam momentum and of the reaction points, and iv) possible wrong assignment of hits to the particle tracks in drift chambers in the case of very close tracks. Some of these, like the multiple scattering, depend on the outgoing proton momenta, others, like the beam momentum distribution, depend on the specific run conditions and therefore must be determined for each run separately. Here we report on the estimations made for the measurement of the $pp \to pp\eta$ reaction at Q = 15.5 MeV.

In order to estimate the variances and covariances for all possible combinations of the momentum components for two registered protons we have generated $1.5 \cdot 10^8$ $pp \to pp\eta$ events and simulated the response of the COSY-11 detection setup taking into account the above listed factors and the known resolutions of the detector components. Next we analysed the signals by means of the same reconstruction procedure as used in case of the experimental data. Covariances between the i^{th} and the j^{th} components of the event vector $(P = [p_{1x}, p_{1y}, p_{1z}, p_{2x}, p_{2y}, p_{2z}])$ were established as the average of the product of the deviations between the reconstruced and generated values. The explicit formula for the sample of N reconstructed events reads:

$$cov(i,j) \;=\; \frac{1}{N}\sum_{k=1}^{N}(P^k_{i,gen} - P^k_{i,recon})(P^k_{j,gen} - P^k_{j,recon}), \qquad (1)$$

where $P^k_{i,gen}$ and $P^k_{i,recon}$ denote the generated and reconstructed values for the i^{th} component of the vector P describing the k^{th} event.

Because of the inherent symmetries of the covariance $(cov(i,j) = cov(j,i))$ and the indistinguishability of the registered protons, there are only 12 independent values which determine the 6 *x* 6 error matrix V unambiguously.

Since inaccuraces of the momentum determination depend on the particle momentum itself (eg. multiple scattering) and on the relative montum between protons (eg. trajectories reconstruction from signals in drift chambers), we have determined the covariance matrices as a function of the absolute momentum of both protons: $cov(i, j, |\vec{p}_1|, |\vec{p}_2|)$.

Below as an example we present the covariance matrix for the mean values of $|\vec{p}_1|$ and $|\vec{p}_2|$ in units of MeV^2/c^2, as established in the laboratory system with the *z*-coordinate parallel to the beam axis and *y*-coordinate corresponding to the vertical direction.

$$V = \begin{array}{c} \begin{array}{cccccc} p_{1x} & p_{1y} & p_{1z} & p_{2x} & p_{2y} & p_{2z} \end{array} \\ \left[\begin{array}{cccccc} 5.6 & 0.0 & -13.7 & 1.7 & 0.1 & -3.0 \\ - & 7.1 & 0.1 & - & -0.2 & -0.2 \\ - & - & 37.0 & - & - & 5.4 \\ - & - & - & - & - & - \\ - & - & - & - & - & - \\ - & - & - & - & - & - \end{array}\right] \end{array} \begin{array}{c} p_{1x} \\ p_{1y} \\ p_{1z} \\ p_{2x} \\ p_{2y} \\ p_{2z} \end{array} \quad (2)$$

Since the measurements have been performed close to the kinematical threshold the ejectile momentum component parallel to the beam is by far the largest one and its variance ($var(p_z) = 37\,MeV^2/c^2$) determines in the first order the error of the momentum measurement. The second largest contribution stems from an anti-correlation between the $x-$ and $z-$ momentum components ($cov(p_x, p_z) = -13.7\,MeV^2/c^2$), which is due to the bending of the proton trajectory – mainly in the horizontal direction – inside the COSY-11 dipole magnet. There is also a significant correlation between the *z* components of different protons which is due to the smearing of the reaction points, namely, if in the analysis the assumed reaction point deviates from the actual one, a mistake made in the reconstruction affects both protons similarly. Figure 10 depict the variation of $var(p_x)$, $var(p_y)$ and $var(p_z)$ over the momentum plane ($|\vec{p}_1|$, $|\vec{p}_2|$).

Taking into account components of the covariance matrices V($|\vec{p}_1|$, $|\vec{p}_2|$) and the distribution of the proton momenta for the $pp \to pp\eta$ reaction at Q = 15.5 MeV results in an average error for the measurement of the proton momentum of about 6 MeV/c. The corresponding distribution is plotted as a dashed line in figure 9(right).

In the experminet we have measured 6 variables and once we assume that the event corresponds to the $pp \to pp\eta$ reaction only 5 of them are independend. Thus we have varied the values of the event component demanding that the missing mass is eqaul to the mass of the η meson and we have chosen that vector which was the closest to the experimental one. The inverse of the covariance matrix was used as a metric for the distance calculation. The kinematical fit improves the resolution by about a factor of 1.5 as can be concluded from the comparison of the dashed and solid lines in figure 9. The finally resulting error of the momentum determination amounts to 4 MeV/c.

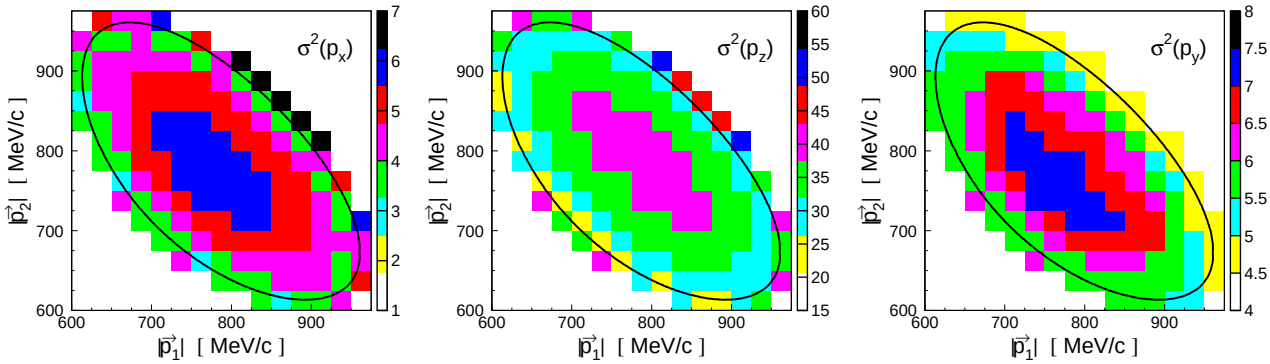

Figure 10: Variances of the protons's momentum components as a function of the absoulte values of the measured momenta.

2.2 Acceptance corrections and results

At the excess energy of Q = 15.5 MeV the COSY-11 detection system does not cover the full 4π solid angle in the centre-of-mass of the $pp \to pp\eta$ reaction. Therefore, the detailed study of the differential cross sections requires the corrections for acceptance. Generally the acceptance should be expressed as a function of the full set of mutually orthogonal variables which describes unambigously the studied reaction. To define the relative movement of the particles in the reaction plane we have chosen two squares of the invariant masses: s_{pp} and $s_{p\eta}$, and to define the orientation of this plane in the center-of-mass frame we have taken the three Euler angles: The first two are simply the polar ϕ^*_η and asimuthal θ^*_η angles of the momentum of the η meson and the third angle ψ describes the turning of the reaction plane around the axis defined by the momentum vector of the η meson. Due to the axial symmetry of the initial channel of the two unpolarized colliding protons the events distribution over ϕ^*_η must be isotropic. Furthermore, taking advantage of the symmetry due to the two identical particles in the initial channel, without losing the generality, we can express the acceptance as a function of s_{pp},$s_{p\eta}$,$|cos(\theta^*_\eta)|$ and ψ. At this representation, however, the COSY-11 detection system covers only 50% of the phase-space for the $pp \to pp\eta$ reaction at Q = 15.5 MeV. To proceed with the analysis we assumed that the distribution over the angle ψ is isotropic as was for example experimentally determined for the $pp \to pp\omega$, $pp \to pp\rho$ or $pp \to pp\phi$ reactions [26, 27]. Please note that this is the only performed assumption about the reaction dynamics in the present evaluation of the data. The validity of this supposition in the case of the $pp \to pp\eta$ reaction will be discussed later.

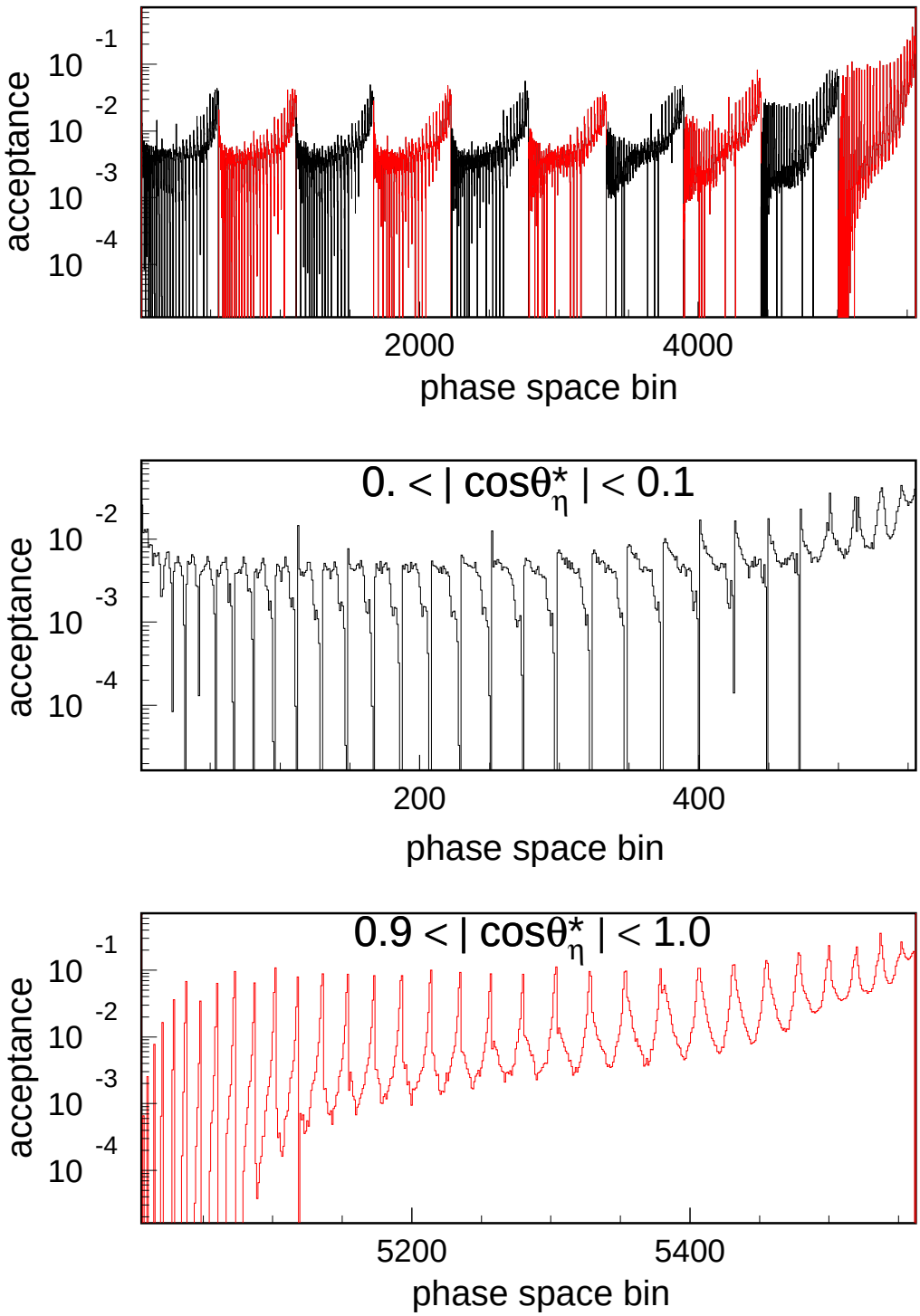

Figure 11: Acceptance of the COSY-11 detection system for the $pp \to pp\eta$ reaction at an excess energy of Q = 15.5 MeV presented as a function of s_{pp},$s_{p\eta}$, and $|cos(\theta^*_\eta|$. The numbers were assigned to the bins in the three dimensional space $s_{pp} - s_{p\eta} - |cos(\theta^*_\eta)|$ by first incrementing the index of s_{pp} next of $s_{p\eta}$ and on the end that of $|cos(\theta^*_\eta)|$. Each second bin of $|cos(\theta^*_\eta)|$ is marked in red. The two pictures below show the acceptance for the first and the last bin of $|cos(\theta^*_\eta)|$.

To facilitate the calculations we have divided the range of $|cos(\theta^*_\eta)|$ into 10 bins and both s_{pp} and $s_{p\eta}$ into 40 bins each. In the case of the s_{pp} and $s_{p\eta}$ the choice was made such that

the width of the interval corresponds to the standrad deviation of the experimental accuracy. For $|cos(\theta^*_\eta)|$ we have taken only ten bins since from the previous experiments we expect only a small variation of the cross section over this variable. In the calculations we utilize also the symmetry of the cross sections under the exchange of the two identical particles in the final state which reads: $\sigma(s_{p_1\eta}, \psi) = \sigma(s_{p_2\eta}, \psi + \pi)$. The resultant acceptance is shown in figure 11. One sees that a small part (3%) of the phase-space is not covered by the detection system. In further calculations these holes were corrected acoording to the assumption of the homogenous phase space distribution. Additionally it was checked that the corrections under other suppositions eg. regarding also the proton-proton FSI leads to negligible differences.

Figure 12(left) presents the distribution of the polar angle of the η meson as derived from the data after the acceptance correction. Within the statistical accuracy it is isotropic. Taking into account this angular distribution of the cross section we can calculated the acceptance as a function of s_{pp} and $s_{p\eta}$ only. This is shown in figure 12(right), where one sees that now the full phase space is covered.

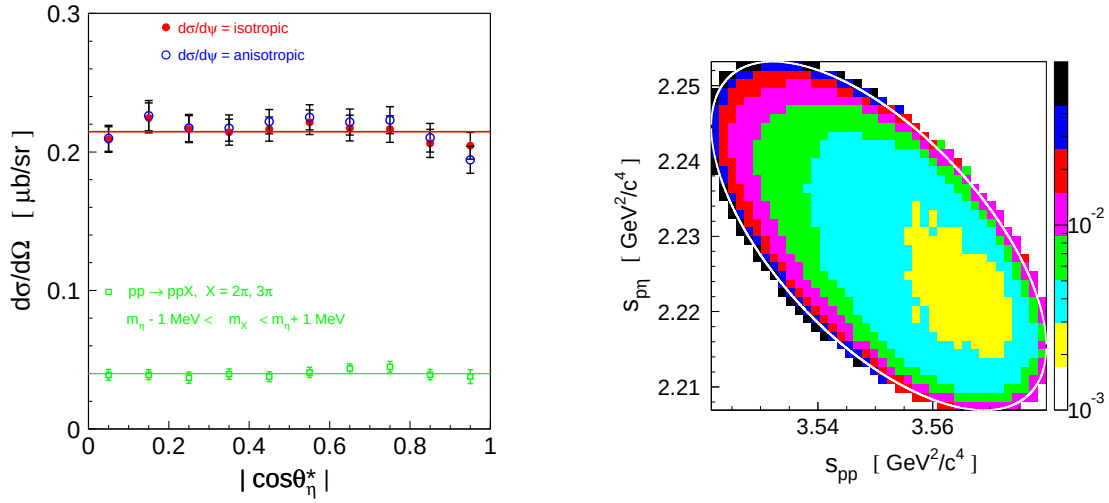

Figure 12: **(left)** Angular distribution determined from the exeperimental date corrected for the acceptance in the three dimensional space $(s_{pp}, s_{p\eta}, |cos(\theta^*_\eta)|)$. Red points show the result with the assumption that the distribution of the ψ angle is isotropic, and the blue ones are extracted under the assumption that $\frac{d\sigma}{d\psi}$ is as derived from the data (see text). Green points presents the result for the multi-pion background under the η signal.
(right) COSY-11 detection acceptnace as a function of s_{pp} and $s_{p\eta}$, calculated under the assumption that the differential cross sections $\frac{d\sigma}{d\cos(\theta^*_\eta)}$ and $\frac{d\sigma}{d\psi}$ are isotropic.

The correctness of the performed procedures for the simulation of the detectors response, the event reconstruction programmes, the kinematical fitting and acceptance correction can be confirmed by comparing the distributions generated (figure 13(left)) with the ones which undergoes the full above mentioned analysis chain (figure 13(right)).

Figure 14 shows the invariant mass distributions for the $pp \to pp\eta$ reaction evaluated at Q = 15.5 MeV after the correction for the detection acceptance. The spectra can be regarded as background free since the number of $pp \to pp\eta$ events was elaborated for each invariant mass interval separately. The exemplarily missing mass spectra corrected for the acceptance are presented in figure 15. From this figure one can infer that the shape of the background is well reproduced not only for the overall

missing mass spectrum as shown previously in figure 8 but also locally in each region of the phase space.

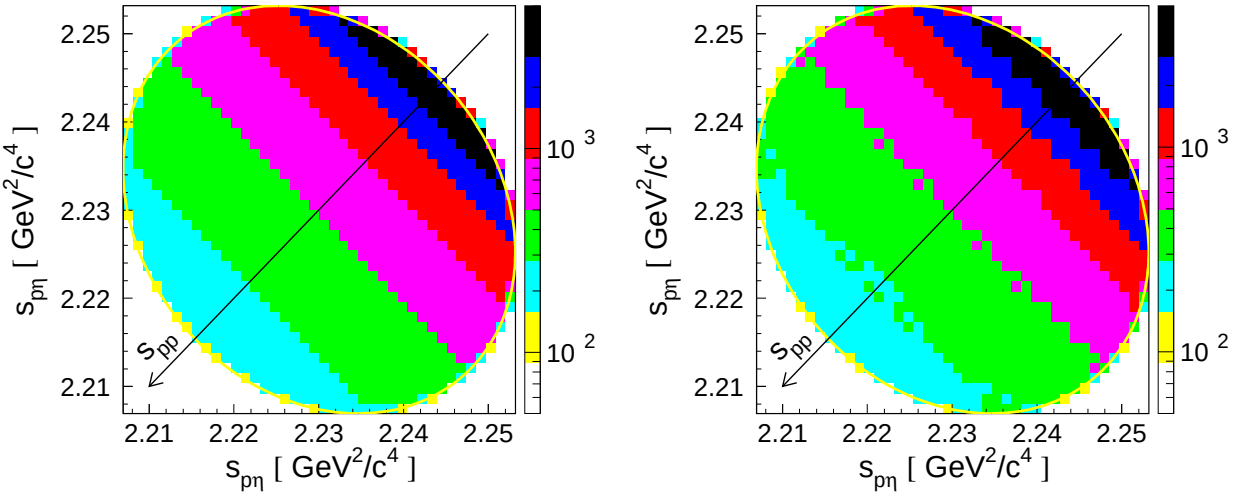

Figure 13: **(left)** Dalitz plot distributions simulated for the $pp \to pp\eta$ reaction at Q = 15.5 MeV. In the calculations the interaction between protons was taken into account. **(right)** Dalitz plot distribution reconstructed from the COSY-11 detector response simulated for events from the left figure taking into account the smearing of the beam and target, multiple scattering in the materials and the detectors resolution. The evaluation included momentum reconstruction, kinematical fitting and the acceptance correction exactly in the same way as performed for the experimental data. The lines surrounding the Dalitz plots depict the kinematical limits.

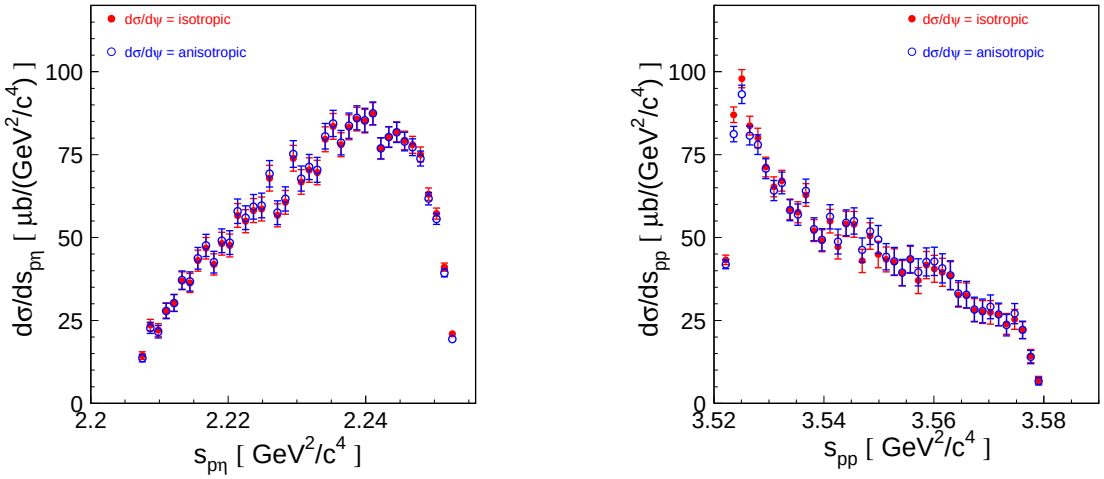

Figure 14: Distributions of the invariant masses s_{pp} and $s_{p\eta}$ determined for the two different assumptions about the cross section dependence on the ψ angle.

Now knowing the distribution of the polar angle of the η meson θ^*_η and those for the invariant masses s_{pp} and $s_{p\eta}$ we can check whether the assumption of the isotropy of the cross section

distribution versus the third Euler's angle ψ is corraborated by the data. For that purpose we have calculated the acceptance as a function of ψ and $s_{p\eta}$ assuming the shape of the differential cross sections of $\frac{d\sigma}{ds_{pp}}$ and $\frac{d\sigma}{dcos(\theta^*_\eta)}$ as determined experimentally. The determined $\frac{d\sigma}{d\psi}$ distribution is depicted by red points in figure 16(left). When fitting to the data a polynomial of the second order one obtains the function which is unisotropic (see red line). To corraborate this observation we have evaluated the distribution over ψ angle (see figure 16(right) from the phase space region which has no holes in the acceptance expressed as a four-dimensional function of the variables s_{pp}, $s_{p\eta}$, $cos(\theta^*_\eta)$ and ψ. Again in agreement with the spectrum determined for all events the obtain distribution is unisotropic and the parameters of the fit are consistent with that from the left panel within the estimated errors. Similarly as in the case of the invariant mass distributions we present in figure 17 exemplarily missing mass spectra which were used to count the number of $pp \to pp\eta$ events for the first, fourth, seventh and tenth interval of ψ values. The experimental data are quite well described by the simulations and thus rather excludes the possibility of a significant systematical error which would cause the observed unisotropy of the differential cross section $\frac{d\sigma}{d\psi}$.

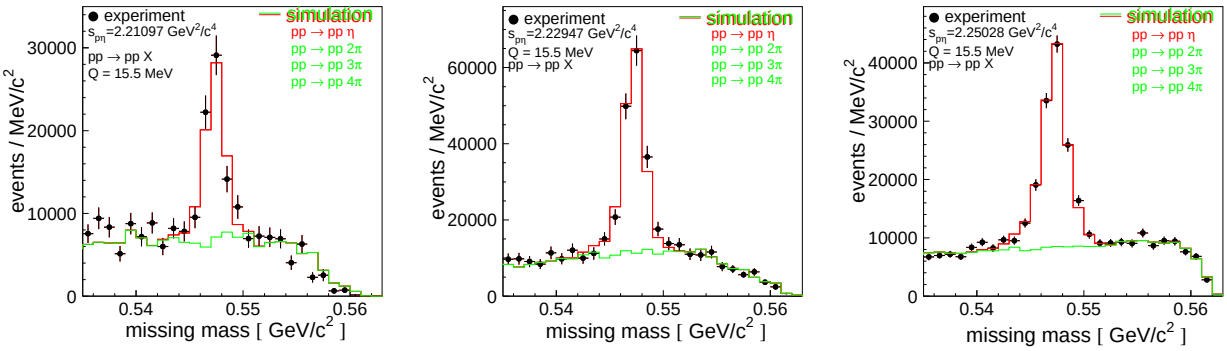

Figure 15: Missing mass distributions determined for the invarian mass bins as depicted inside the figures. The red and green histograms shows the simulated spectra for the $pp \to pp\eta$ and $pp \to pp(n\pi)$ reactions fitted to the data with the amplitudes as the only free parameters.

Since in the analysis we have anticipated that this distribution is isotropic we have repeated the full calculation now assuming that the differential cross section $\frac{d\sigma}{d\psi}$ is as determined from the data. The result of the newly established distributions are compared to the former results in figures 12(left), 14 and are shown as green points in figure 16. From that comparison one can conclude that the shapes of the determined distributions are -within the statistical accuracy - independend of the shape of the $\frac{d\sigma}{d\psi}$ cross section and can be treated as derived in a completely model independent manner.

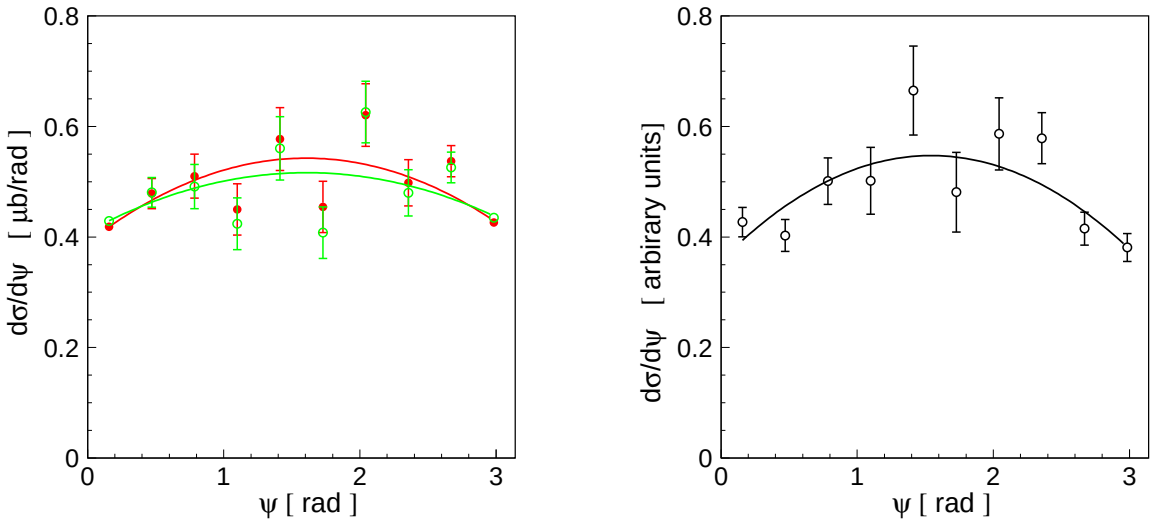

Figure 16: Distribution of the cross section as a function of the angle ψ defined in the text. **(left)** For the $pp \to pp\eta$ reaction for all data. **(right)** Only data from the left upper edge of the Dalitz plot have been taken into account (see for example figure 12(right)). At that region of the Dalitz plot due to the non zero four dimensional acceptance over (s_{pp}, $s_{p\eta}$, $|cos(\theta^*_\eta)|$,ψ) bins the spectrum was corrected without a necessity of any assumption concerning the reaction cross section.

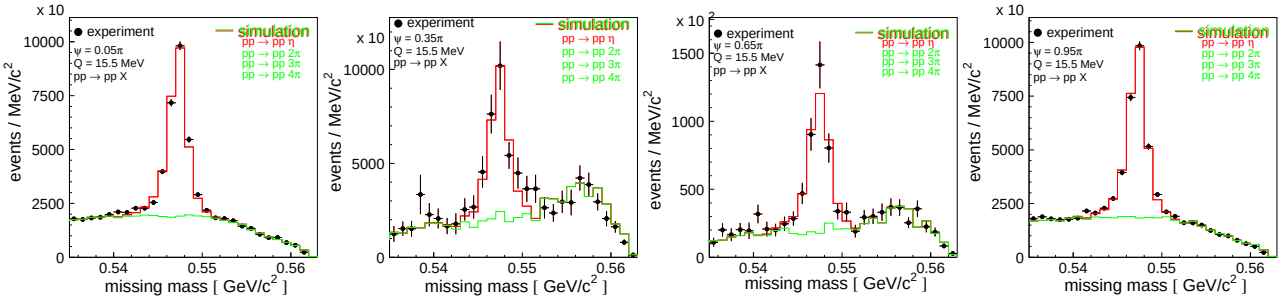

Figure 17: Missing mass distributions for the first, fourth, seventh and tenth bin of ψ with the superimposed lines from the simulation of $pp \to pp\eta$ and $pp \to pp(n\pi)$ reactions.

3 Estimation of the requested beam-time

During the 7 days of the measurement performed in the year 2000 we have registered and reconstructed 24000 events corresponding to the $pp \to pp\eta$ reaction. This means about 3420 events per day. For the estimation of the rate of $pp \to pp\eta'$ reaction we have considered the following factors:

The COSY-11 detection system acceptance for the $pp \to pp\eta'$ reaction is by a factor of 2.3 larger than that for the reaction $pp \to pp\eta$ at the same excess energy. This is because the center of mass of the $pp \to pp\eta'$ reaction is moving much faster than the one for $pp \to pp\eta$ reaction, and consequently the cone of the reaction products in the laboratory is smaller and hence larger fraction of events can be registered.

The total cross section for the $pp \to pp\eta'$ reaction is by factor 30 smaller than that for the reaction $pp \to pp\eta$.

Finally taking into account the increase of the COSY beam intensity within the last three years by a factor of 1.5 to 2.5 we estimate to register about $\frac{3420 \cdot 2.3 \cdot 2}{30} \approx 520$ $pp \to pp\eta'$ events per day.

In order to measure the invariant mass spectra for the $pp \to pp\eta'$ reaction with the statistics comparable to the measurements for the meson η we would like to ask for four weeks of the COSY beam operation with a momentum of 3.257 GeV/c equivalent to the excess energy of Q = 15.5 MeV. This would allow us to register about 14000 events.

References

[1] S. Wycech, private communication;
A. Fix, private communication;
V. Baru, private communication;
K. Nakayama, private communication;
J. Haidenbauer, C. Hanhart, H. Garcilazo, private communication

[2] P. Moskal, M. Wolke, A. Khoukaz, W. Oelert,
Prog. Part. Nucl. Phys. **49** (2002) 1,
e–Print Archive hep-ph/0208002.

[3] F. Balestra et al., Phys. Lett. **B 491** (2000) 29.;
P. Moskal et al., Phys. Lett. **B 474** (2000) 416.;
P. Moskal et al., Phys. Rev. Lett. **80** (1998) 3202.;
A. Khoukaz et al., Ann. Rep. 2001, IKP Uni. Münster

[4] F. Hibou et al., Phys. Lett. **B 438** (1998) 41.;

[5] H. Calén et al., Phys. Lett. **B 366** (1996) 39.;
J. Smyrski et al., Phys. Lett. **B 474** (2000) 182.;
E. Chiavassa et al., Phys. Lett. **B 322** (1994) 270.;
A. M. Bergdolt et al., Phys. Rev. **D 48** (1993) R2969.;
H. Calén et al., Phys. Rev. Lett. **79** (1997) 2642.;

[6] G. Fäldt and C. Wilkin, Phys. Lett. **B 382** (1996) 209.

[7] A. M. Green, S. Wycech, Phys. Rev. **C 55** (1997) R2167.

[8] P. Moskal et al., Phys. Lett. **B 482** (2000) 356.

[9] D. Sigg et al., Nucl. Phys. **A 609** (1996) 269.

[10] J. P. Naisse, Nucl. Phys. **A 278** (1977), 506.

[11] H. O. Meyer et al., Nucl. Phys. **A 539** (1992) 633. and Phys. Rev. Lett. **65** (1990) 2846.; A. Bondar et al., Phys. Lett. **B 356** (1995) 8.

[12] D.E. Groom et al., Eur. Phys. J. **C 15** (2000) 1.

[13] V. Hejny et al., Eur. Phys. J. **A 13**, 493 (2002).; Ch. Elster et al., e-Print Archive: nucl-th/0207052.

[14] J. Dyring, Ph.D. thesis, University of Uppsala, Acta Universitatis Upsaliensis **14** (1997)

[15] M. Abdel-Bary et al., Eur. Phys. J. **A 16** (2003) 127.

[16] H. P. Noyes, H. M. Lipinski, Phys. Rev. **C 4** (1971), 995.

[17] K. Nakayama et al., e-Print Archive: nucl-th/0302061.

[18] V. Baru et al., Phys. Rev. **C 67** (2003) 024002.

[19] J. Złomańczuk et al., Phys. Lett. **B 436** (1998) 251.

[20] R. Bilger et al., Nucl. Phys. **A 693** (2001) 633.

[21] H.O. Meyer et al., Phys. Rev. **C 63** (2001) 064002.

[22] S. Brauksiepe et. al., Nucl. Instr. & Meth. **A 376** (1996) 397.

[23] D. Prasuhn et al, Nucl. Instr. & Meth. **A 441** (2000) 167.

[24] H. Dombrowski et al., Nucl. Instr. & Meth. **A 386** (1997) 228.

[25] P. Moskal et al, Nucl. Instr. & Meth **A 466** (2001) 448.

[26] F. Balestra et al., Phys. Rev. Lett. **89** (2002) 092001.

[27] J. Ritman, Habilitation thesis, Gießen University (2000).